

Optically stimulated luminescence dating of the upper horizon of a Serbian loess-paleosoil sequence using quartz

Anca AVRAM^{1,2,*}, Marius MANDROC¹, Daniela CONSTANTIN^{1,2}, Slobodan MARKOVIĆ³, Alida TIMAR-GABOR^{1,2}

¹ Faculty of Environmental Science and Engineering, Babes-Bolyai University, Cluj-Napoca, Romania

² Interdisciplinary Research Institute on Bio-Nano-Sciences, Environmental Radioactivity and Nuclear Dating Centre, Babes-Bolyai University, Cluj-Napoca, Romania

* Corresponding author: A. Avram, email: anca.avram92@gmail.com

Abstract

Optically stimulated luminescence dating widely used for establishing high-resolution chronologies for the Quaternary in paleoclimate research. Loess is an important archive of past climate changes on continents. In order to provide a first absolute chronology for Zemun loess paleosoil sequence in Serbia, the single-aliquot-regenerative dose (SAR) protocol was applied on coarse (63-90 μm) quartz fraction extracted from five samples. The profile reaches a thickness of 4 m, where the modern soil is visible in the uppermost part of the section. The investigated samples were collected from the transition between the uppermost visible soil and the loess layer, based on field observations. The results of the SAR-OSL protocol intrinsic rigor tests indicate that it can be successfully applied on coarse quartz extracted from Zemun samples, as all the results were within accepted limits of variation. The equivalent doses determined range from 13.8 ± 1.5 Gy (ZMN 55A) to 20.5 ± 2.1 Gy (ZMN 75A). Thus, the luminescence ages obtained for the investigated samples vary between 5.8 ± 0.8 ka (ZMN 55A) and 8.7 ± 1.1 ka (ZMN 75A). According to the ages obtained all the samples are assigned to the Holocene period.

Key words: luminescence dating, quartz, loess, SAR protocol, OSL ages

INTRODUCTION

The future environment trajectories may be predicted if the past conditions are very well known. Fortunately, the terrestrial surface of the Earth has the ability to preserve information about the past climatic conditions that guided the development of human species and their habitat. One of the most important terrestrial archives that was able to record the past climatic conditions is represented by loess deposits which are distributed over 10% of the world's continents and even more in some parts of Eurasia (Pécsi 1990). Since loess-paleosol sequences are considered one of the most continuous and extensive terrestrial archives of the climate variability during Quaternary, they have a key role in assessing the landscape dynamics and global dust cycle (Schatzel et al., 2018; Lehmkuhl et al., 2021). The specific characterisation of loess and paleosol alternations are related to climatic fluctuations. As such, loess units were formed during relatively dry-cool conditions whereas paleosol units were developed during a warm-humid period; all these are correlated with glacial-interglacial variability. In general, their timing is assumed to be simultaneous with the major climate changes that are very well documented in ice core and marine records (Bazin et al., 2013; Govin et al., 2015). In order to interpret the information recorded in these archives, the moment when the sediment

was deposited should be assessed. Luminescence dating is an established method for this purpose. This technique uses minerals that are able to store charge upon irradiation in time. The energy accrued by the mineral due to natural occurring radioactivity can be released in the form of light and is represented by a signal in the form of a luminescence signal. This signal increases with the exposure to radioactivity in time and can be erased by exposure to light or heat. Since the first application of the Optically Stimulated Luminescence (OSL) dating on quartz (**Huntley et al., 1985**), technological improvements made during the last decades have contributed in significant developments on the accuracy and precision of this method. OSL dating using Single Aliquot Regenerative dose (SAR) protocol (**Murray and Wintle 2000, 2003**) is regarded as the most powerful dating methods that can establish absolute chronologies for loess deposits all over the world (e.g., **Marković et al., 2014; Timar-Gabor et al., 2015; Constantin et al., 2014; Veres et al., 2018; Tecsá et al., 2020a, b; Avram et al., 2020, 2022; Brezeanu et al., 2021**).

Loess-paleosol sequences in the Carpathian Basin in the form of dust deposition and soil formation during the Quaternary period, are known to provide information on the climatic variability in this region (**Fuchs et al., 2008; Marković et al., 2008; Stevens et al., 2011**). The province of Vojvodina is situated in the northern Serbia and represents a lowland part of the southern Carpathian Basin. This region encompasses the confluence area of the Danube, Tisa and Sava rivers (**Marković et al., 2008**). Loess-paleosol sequences in the Vojvodina region are considered as one of the most extensive, complete and thickest terrestrial archives that were able to record past climatic events since the Pleistocene (**Marković et al., 2015**). OSL dating method has been successfully applied on several loess-paleosol sequences from Vojvodina region, such as: Stari Slankamen (**Murray et al., 2014**); Orlovat (**Timar-Gabor et al., 2015**); Mošorin (**Constantin et al., 2019**); Batajnica (**Avram et al., 2020**); Kisiljevo (**Péric et al., in press**); Smederevo (**Constantin et al., 2021**). The aim of this study is to assess the applicability of the OSL dating technique using the standard SAR protocol on quartz extracted from a loess deposit located in the Vojvodina region, Serbia, and to establish an absolute time frame for loess deposition using samples collected at the Pleistocene/Holocene transition as expected based on field observations.

SAMPLING AND SITE DESCRIPTION

The loess profile (44° 51' 29" N and 20° 23' 13"E) investigated in this study (Zemun) is situated along the Danube in the Vojvodina region, in the north-western part of the outskirts of Belgrade in northern Serbia (**Figure 1**). The sequence exhibits a thickness of approximately 4 m. Based on the field observations, the upper part of the profile with a thickness of 0.7 m represents the modern soil. At a depth of 50 cm, many krotovinas were observed.

Since the upper part of the profile exposure allows investigating the Pleistocene/Holocene transition, the study site represents an important archive for dating the moment of the transition. Therefore, in the attempt to date the Pleistocene/Holocene transition, as recorded by field observations, five individual samples were collected and prepared for luminescence investigations. Based on the field observation, samples ZMN 55A and ZMN 65A were collected from the modern soil, denoted as S0, while ZMN 75A and ZMN 85A were sampled in order to match the transition. Moreover, a sample from L1 unit ZMN 95A was also collected.

OPTICALLY STIMULATED LUMINESCENCE DATING

Sample preparation

Five luminescence samples were collected in stainless steel tubes and prepared under subdued red light laboratory conditions. In order to avoid the contamination, the material from the end of each tube was removed and used for gamma spectrometry analysis. Quartz minerals were extracted from the material left in the inner part of the tube. First step of sample preparation consisted in a chemical treatment with hydrochloric acid of 10% concentration and hydrogen peroxide with a concentration of 30%, respectively. As a result, carbonates and organic matter were completely removed. Further, the sediment was separated into finer (<63 µm) and coarser (>63 µm) material through dry sieving. The grain size of interest (63-90 µm) was obtained from the coarser material by sieving. Due to the small amount of coarse material, the density separation with heavy liquid could not be performed. To isolate quartz grains from the plagioclase feldspars, a prolong treatment with hydrofluoric acid (40% concentration for 1 hour) has been performed. To remove the precipitated fluorides, a rinse with hydrochloric acid (10% concentration) for 60 minutes has been carried out. In order to perform the luminescence measurements, the coarse quartz grains were mounted on stainless steel discs using silicon oil as an adhesive.

Analytical facilities

Luminescence investigations were performed using two TL/OSL Risø DA-20 readers equipped with an automated detection and stimulation head (DASH) (**Lapp et al., 2015**). The intensity of the blue (470 nm) and infrared (870 nm) stimulation diodes are ~80 and ~300 mW/cm², respectively. Luminescence signal detection was made by using a PDM 9107Q-AO-TTL-30 (160-630 nm) photomultiplier tube (**Thomsen et al., 2006**). Quartz signals were detected by 7.5-mm-thick Hoya U-340 UV filter. Laboratory irradiations were performed using the incorporated ⁹⁰Sr-⁹⁰Y radioactive sources that were calibrated with gamma-irradiated calibration quartz (**Hansen et al., 2015**). The dose rate of coarse quartz measured on the automated DASH reader was ~0.09 Gy/s.

Equivalent dose determination

Equivalent doses on coarse quartz were measured using a standard single aliquot regenerative dose (SAR) protocol (**Murray and Wintle, 2000, 2003**). The protocol is outlined in **Table 1**. Blue-light emitting diodes were used for the optical stimulation which was carried out for 40 s at a temperature of 125 °C. In order to reduce the contribution of the slow and medium components, the net continuous wave optically stimulated luminescence (CW-OSL) signal of interest was integrated over the first 0.308 s of the decay curve minus an early background (**Cunningham and Wallinga, 2010**). Sensitivity change correction was made by using the OSL response to a test dose of 17 Gy. A preheat temperature of 220 °C for 10 s and a cutheat of 180 °C were employed. A high-temperature bleach (at 280 °C for 40 s) was performed at the end of each SAR cycle using blue diodes as stimulation source (**Murray and Wintle, 2003**).

In order to assess the robustness of the SAR protocol, the intrinsic performance tests (recycling and recuperation) (**Murray and Wintle 2003**) were integrated in every measurement. The purity of quartz luminescence signals was checked through the IR depletion test that consisted of adding an IR stimulation step prior to OSL measurement in the last cycle of the SAR protocol (**Duller, 2003**). Recycling and IR

depletion ratios within 10% deviation from unity constituted the acceptance criteria for aliquots that were used in equivalent dose determination. Recuperation ratio was considered suitable if the value of the signal measured after a zero dose was less than 2% of the natural signal.

Dosimetry

Radionuclide activity concentrations were determined by using a high-resolution gamma spectrometry. The measurements were carried out using a well-type HPGe detector. Samples were stored for one month in order to reach equilibrium between ^{226}Ra and its parent ^{222}Rn . The total dose rates were derived based on the conversion factors tabulated by **Guérin et al. (2011)**. Based on the average humidity of loess samples in Vojvodina region, a time-average water content of 15% with an assumed relative error of 25% was used (e.g., **Avram et al., 2020**). A factor of 0.94 ($\pm 5\%$ error) was assumed to correct the external beta dose rates for the effects of attenuation and etching (**Mejdhal, 1979**) and following the recommendation of **Vandenberghé et al. (2008)** an internal dose rate of $0.010 \pm 0.002 \text{ Gy ka}^{-1}$ was adopted for the coarse fraction. The cosmic ray contribution to the total dose rate was calculated based on the formula tabulated by **Prescott and Hutton (1994)** using depth, altitude, latitude and longitude for each sample. Relevant information about the uranium, thorium and potassium concentration along with the cosmic dose rates are labelled in **Table 2** while the annual doses are displayed in **Table 3**.

RESULTS AND DISCUSSIONS

Luminescence properties of quartz

The net signals of coarse quartz decay significantly within the first seconds of optical stimulation as documented for sample ZMN 55A in the inset of **Figure 2**. The pattern exhibited by the natural and regenerated decay curves of coarse quartz appear indistinguishable with that measured for calibration quartz, which is accepted to be dominated by the fast component (**Hansen et al., 2015**).

Representative SAR laboratory growth curve constructed for a single aliquot of 63-90 μm quartz from sample ZMN 55A is displayed in **Figure 2**. The dose response curves were well described by a sum of two saturating exponential function. Ratios within 10% from unity were obtained for recycling and IR depletion ratios. These results demonstrate that the sensitivity changes during the repeated SAR cycles are properly corrected for, and that the investigated signals come from quartz and no other contaminant minerals.

Dose recovery test

The single and most complete test that characterise the performance of the SAR procedure for any given sample is the dose recovery test (**Murray and Wintle 2003**). It is used to assess whether the SAR protocol can accurately measure a known dose administered prior to any thermal treatment. Sets of five aliquots of 63-90 μm quartz from samples ZMN 55A and ZMN 95A were used. The natural signals were first removed by a double exposure to blue light emitting diodes for 100 s at room temperature with a pause of 10 ks. Further, the aliquots were irradiated with laboratory beta doses chosen to be similar to equivalent doses. The given dose is then measured using the SAR protocol in the same manner as the equivalent doses. The dose recovery ratio was further calculated by dividing the recovered to the given dose. The value of the dose recovery ratio should be close to unity. The results of

the dose recovery test are presented in **Figure 3**. As can be seen, for sample ZMN 55A, a dose recovery ratio of 0.95 ± 0.02 was calculated whereas for sample ZMN 95 A, a ratio of 0.97 ± 0.02 was obtained. These results suggested that the SAR protocol can successfully measure the doses over the interval investigated here.

Equivalent doses

Equivalent doses were determined by projecting the sensitivity corrected natural luminescence signal onto the dose response curve constructed for each sample investigated (**Figure 2**). 10 replicate measurements were carried out for each sample in order to calculate the equivalent dose. **Table 3** summarises the measured equivalent dose for each sample as well as the results of the intrinsic tests of the SAR protocol (Recycling, IR depletion and Recuperation). The obtained equivalent doses range from 14 ± 2 Gy for sample ZMN 55A to 21 ± 2 Gy for sample ZMN 75A.

Luminescence ages

OSL ages are represented in **Table 3** and **Figure 4** as function of depth. As can be seen, for the uppermost sample collected from a depth of 55 cm an age of 5.5 ± 0.7 ka (ZMN 55A) was obtained, whereas for the sample collected from a depth of 95 cm an age of 7.4 ± 1.0 ka (ZMN 95A) was calculated. In this depth interval of sample collection, the oldest age (9.3 ± 1.2 ka) was obtained for sample ZMN 75A. As can be seen, the ages are increasing with depth up to sample ZMN 75A while for samples ZMN 85 A and ZMN 95 A the ages are smaller. The age inversion is often encountered in the upper parts of loess-paleosol profiles and it is considered to be the effect of the paedogenetic process (e.g., **Constantin et al., 2021**).

DISCUSSION AND CONCLUSIONS

As far as methodological dating investigations are concerned, Optically Stimulated Luminescence dating has been successfully applied on quartz samples investigated in this study. The sensitivity corrected luminescence signal of 63-90 μm quartz was shown to be dominated by the fast component and thus exhibiting the optimal characteristics for the application of the SAR protocol. The robustness of the applied protocol has been assessed through the intrinsic tests, namely: Recycling, Recuperation and IR depletion test. The results of these tests were within the acceptability criteria, demonstrating the robustness of the protocol.

The aim of this study was to provide absolute luminescence ages for 5 loess samples collected from Zemun loess sequence located in Vojvodina region in order to establish the moment of the Pleistocene/Holocene transition as assigned by field observations only. For the samples collected in this regard, the OSL ages increase up to an age of 9.3 ± 1.2 ka obtained for sample ZMN 75A. This sample was thought to be collected exactly from the depth where the Pleistocene/Holocene transition was identified in the field. The timing of the Pleistocene/Holocene boundary defined in ice-core records is 11.7 ka (**Rasmussen et al., 2014; Walker et al., 2019**). A recent study conducted by **Constantin et al. (2021)** investigated the moment of Pleistocene/Holocene transition as recorded by variations of the magnetic susceptibility in loess worldwide, concluding that the timing of the Pleistocene-Holocene climatic transition, as recorded by this proxy is prior to 11.7 ka, around 14-17.5 ka. Our results show a mismatch between the chronological information obtained by luminescence dating and the field information collected during the sampling. As such, for this particular section our results highlight the need for dating

more samples collected at larger depths as well as the necessity of carrying out magnetic susceptibility measurements. Overall, this study demonstrated that stratigraphic boundaries and their associated climatic transitions cannot be accurately identified in loess-paleosoil sequences based on field observations only, highlighting the need for using proxies and the application of absolute dating methods.

ACKNOWLEDGEMENTS

This study was funded by the European Research Council (ERC) under the European Union's Horizon 2020 research and innovation programme ERC-2015-STG, (grant agreement No [678106]).

Anca Avram and Alida Timar-Gabor received financial support of the research project EEA-RO-NO-2018-0126.

REFERENCES

- Aitken M. J., Alldred J. C., 1972, The assessment of error limits in thermoluminescent dating. *Archaeometry* **14**, pp. 257–267.
- Avram A., Constantin D., Veres D., Kelemen S., Obreht I., Hambach U., Marković S. B., Timar-Gabor A., 2020, Testing polymineral post-IR IRSL and quartz SAR-OSL protocols on Middle to Late Pleistocene loess at Batajnica, Serbia. *Boreas* **49**, pp. 615–633.
- Avram A., Constantin D., Hao Q., Timar-Gabor A., 2022, Optically stimulated luminescence dating of loess in South-Eastern China using quartz and polymineral fine grains. *Quat. Geochronol.* **67**, pp. 101226.
- Bazin L., Landais A., Lemieux-Dudon B., Toyé Mahamadou Kele H., Veres D., Parrenin F., Martinerie P., Ritz C., Capron E., Lipenkov V., Loutre M. F., Raynaud D., Vinther B., Svensson A., Rasmussen S., Severi M., Blunier T., Leuenberger M., Fischer H., Masson-Delmotte V., Chappellaz J., Wolff E., 2013, An optimized multi-proxy, multi-site Antarctic ice and gas orbital chronology (AICC2012): 120-800 ka. *Clim. Past* **9**, pp. 1715–1731.
- Brezeanu D., Avram A., Micallef A., Cinta Pinzaru S., Timar-Gabor A., 2021, Investigations on the luminescence properties of quartz and feldspars extracted from loess in the Canterbury Plains, New Zealand South Island. *Geochronometria* **48**, pp. 46-60.
- Constantin D., Begy R., Vasiliniuc S., Panaiotu C., Necula C., Codrea V., Timar-Gabor A., 2014, High-resolution OSL dating of the Costinesti section (Dobrogea SE Romania) using fine and coarse quartz. *Quat. Int.*, **334-335**, pp. 20-29.
- Constantin D., Veres D., Panaiotu C., Anechitei-Deacu V., Groza S. M., Begy R. C., Kelemen S., Buylaert J. P., Hambach U., Marković S. B., Gerasimenko N., Timar-Gabor, A., 2019, Luminescence age constraints on the Pleistocene-Holocene transition recorded in loess sequences across SE Europe. *Quat. Geochronol.* **49**, pp. 71–77.
- Constantin D., Mason J. A., Veres D., Hambach U., Panaiotu C., Zeeden C., Zhou L., Marković S.B., Gerasimenko N., Avram A., Tecsa V., Groza-Sacaciu S. M., del Valle Villalonga L., Begy R., Timar-Gabor A., 2021, *Earth-Sci. Rev.*, **221**, pp. 103769.
- Cunningham A. C., Wallinga J., 2010, Selection of integration time intervals for quartz OSL decay curves. *Quat. Geochronol.* **5**, pp. 657–666.

- Duller G. A. T., 2003, Distinguishing quartz and feldspars in single grain luminescence measurements. *Radiat. Meas.* **37**, pp. 161–165.
- Fuchs M., Rousseau D. D., Antoine P., Hatté C., Gauthier C., Marković S. B., Zoeller L., 2008, High resolution chronology of the upper Pleistocene loess/paleosol sequence at Surduk, Vojvodina, Serbia. *Boreas* **37**, pp. 66–73.
- Govin A., Capron E., Tzedakis P.C., Verheyden S., Ghaleb B., Hillaire-Marcel C., St-Onge G., Stoner J. S., Bassinot F., Bazin L., Blunier T., Combourieu-Nebout N., El Ouahabi A., Genty D., Gersonde R., Jimenez-Amat P., Landais A., Martrat B., Masson-Delmotte V., Parrenin F., Seidenkrantz M.-S., Veres D., Waelbroeck C., Zahn R., 2015, Sequence of events from the onset to the demise of the last Interglacial: evaluating strengths and limitations of chronologies used in climatic archives. *Quat. Sci. Rev.* **129**, pp. 1–36.
- Guérin G., Mercier N., Adamiec G., 2011, Dose-rate conversion factors: update. *Ancient TL* **29**, pp. 5–8.
- Haase D., Fink J., Haase G., Ruske R., Pécsi M., Richter H., Altermann M., Jager K. D., 2007, Loess in Europe - its spatial distribution based on a European Loess Map, scale 1:2,500,000. *Quat. Sci. Rev.* **26**, pp. 1301–1312.
- Hansen V., Murray A., Buylaert J. P., Yeo E. Y., Thomsen K., 2015, A new irradiated quartz for beta source calibration. *Radiat. Meas.* **81**, pp. 123–127.
- Huntley D. J., Godfrey-Smith, D. I., Thewalt M. L. W., 1985, Optical dating of sediments. *Nature* **313**, pp. 105–107.
- Lapp T., Kook M., Murray A. S., Thomsen K. J., Buylaert J. P., Jain M., 2015, A new luminescence detection and stimulation head for the Risø TL/OSL reader. *Radiation Measurements* **81**, pp. 178–184.
- Lehmkuhl F., Nett J. J., Pötter S., Schulte P., Sprafke T., Jary Z., Antoine P., Wacha L., Wolf D., Zerboni A., Hösek J., Marković S. B., Obrecht I., Sümegi P., Veres D., Zeeden C., Boemke B., Schaubert V., Viehweger J., Hambach U., 2021, Loess landscapes of Europe—Mapping, geomorphology, and zonal differentiation. *Earth Sci. Rev.* 103496.
- Marković SB, Bokhorst MP, Vandenberghe J, et al. 2008. Late Pleistocene loess–paleosol sequences in the Vojvodina region, north Serbia. *Journal of Quaternary Science* 23: 73–84.
- Marković S. B., Timar-Gabor A., Stevens T., Hambach U., Popov D., Tomić N., Obrecht I., Jovanović M., Lehmkuhl F., Kels H., Marković R., Gavrilov M. B., 2014, Environmental dynamics and luminescence chronology from the Orlovat loess-paleosol sequence (Vojvodina, northern Serbia). *J. Quat. Sci.* **29**, pp. 189–199.
- Marković S. B., Stevens T., Kukla G. J., Hambach U., Fitzsimmons K., Gibbard P., Buggle B., Zech M., Guo Z., Hao Q., Wu H., O'Hara-Dhand K., Smalley I., Ujvari G., Sümegi P., Timar-Gabor A., Veres D., Sirocko F., Vasiljevic D., Svircev Z., 2015, Danube loess stratigraphy – Towards a pan-European loess stratigraphic model. *Earth-Sci. Rev.* **148**, pp. 228–258.
- Mejdahl V., 1979, Thermoluminescence dating: beta-dose attenuation in quartz grains. *Archaeometry* **21**, pp. 61–72.
- Murray A. S., Wintle A. G., 2000, Luminescence dating using an improved single-aliquot regenerative-dose protocol. *Radiat. Meas.* **32**, pp. 57–73.
- Murray A. S., Wintle A.G., 2003, The single aliquot regenerative dose protocol: potential for improvements in reliability. *Radiat. Meas.* **37**, pp. 377–381.

- Murray A. S., Schmidt E. D., Stevens T., Buylaert J.-P., Marković S. B., Tsukamoto S., Frechen M., 2014, Dating Middle Pleistocene loess from Stari Slankamen (Vojvodina, Serbia) – Limitations imposed by the saturation behaviour of an elevated temperature IRSL signal. *Catena* **117**, pp. 34–42.
- Pécsi M., 1990, Loess is not just the accumulation of dust. *Quat. Int.*, **7-8**, pp. 1-21.
- Perić Z. M., Marković S. B., Avram A., Timar-Gabor A., Zeeden C., Nett J. J., Fischer P., Fitzsimmons K. E., Gavrilov M. B., *Quat. Int.*, in press., <http://dx.doi.org/10.1016/j.quaint.2020.10.040>.
- Prescott J. R., Hutton J. T., 1994, Cosmic ray contributions to dose rates for luminescence and ESR dating: large depths and long term variations. *Radiat. Meas.* **23**, pp. 497–500.
- Rasmussen S. O., Bigler M., Blockley S. P., Blunier T., Buchardt S. L., Clausen H. B., Cvijanovic I., Dahl-Jensen D., Johnsen S. J., Fischer H., Gkinis V., Guillevic M., Hoek W. Z., Lowe J. J., Pedro J. B., Popp T., Seierstad I. K., Steffensen J. P., Svensson A. M., Vallelonga P., Vinther B. M., Walker M. J. C., Wheatley J. J., Winstrup M., 2014. A stratigraphic framework for abrupt climatic changes during the last Glacial period based on three synchronized Greenland ice-core records: refining and extending the INTIMATE event stratigraphy. *Quat. Sci. Rev.* **106**, pp. 14–28.
- Schaetzl R. J., Bettis E. A., Crouvic O., Fitzsimmons K. E., Grimley D. A., Hambach U., Lehmkuhl F., Marković S. B., Mason J. A., Owczarek P., Roberts H. M., Rousseau D. D., Stevens T., Vandenberghe J., Zarate M., Veres D., Yang S. L., Zech M., Conroy J. L., Dave A. K., Faust D., Hao Q. Z., Obrecht I., Prud'homme C., Smalley I., Tripaldi A., Zeeden C., Zech R., 2018, Approaches and challenges to the study of loess - introduction to the Loess-Fest. *Quat. Res.* **89**, pp. 563–618.
- Stevens T., Marković S. B., Zech M., Hambach U., Sümegi P., 2011, Dust deposition and climate in the Carpathian Basin over an independently dated last glacial–interglacial cycle. *Quat. Sci. Rev.* **30**, pp. 662–681.
- Tecsa V., Gerasimenko N., Veres D., Hambach U., Lehmkuhl F., Schulte P., Timar-Gabor A., 2020a, Revisiting the chronostratigraphy of late Pleistocene loess-paleosequences in southwestern Ukraine: OSL dating of Kurortnesection. *Quat. Int.* **542**, pp. 65–79.
- Tecsa V., Mason J.A., Johnson W.C., Miao X., Constantin D., Radu S., Magdas D.A., Veres D., Marković S. B., Timar-Gabor A., 2020b, Late Pleistocene to Holocene loess in the central Great Plains: Optically stimulated luminescence dating and multi-proxy analysis of the Enders section (Nebraska, USA). *Quat. Sci. Rev.* **229**, pp. 106130.
- Thomsen K. J., Bøtter-Jensen L., Denby P. M., Moska P., Murray A. S., 2006, Developments in luminescence measurement techniques. *Radiat. Meas.* **41**, pp. 768–773.
- Timar-Gabor A., Constantin D., Marković S. B., Jain M., 2015, Extending the area of investigation of fine versus coarse quartz optical ages from the Lower Danube to the Carpathian Basin. *Quat. Int.*, **388**, pp. 168-176.
- Vandenberghe D. A. G., De Corte F., Buylaert J.-P., Küçera J., Van den Haute P., 2008, On the internal radioactivity in quartz. *Radiat. Meas.* **43**, pp. 771–775.
- Veres D., Tecsa V., Gerasimenko N., Zeeden C., Hambach U., Timar-Gabor A., 2018, Short-term soil formation events in last glacial east European loess,

evidence from multi-method luminescence dating. *Quat. Sci. Rev.* **200**, pp. 34–51.

Walker M., Head M. J., Lowe J., Berkelhammer M., Björck S., Cheng H., Cwynar L., Fisher D., Gkinis V., Long A., Lowe J., Newnham R., Rasmussen S., Weiss H., 2019, Subdividing the Holocene Series/Epoch: formalization of stages/ages and subseries/subepochs, and designation of GSSPs and auxiliary stratotypes. *J. Quat. Sci.* **34**, pp. 173–186.

Table 1. Flowchart of the Single Aliquot Regenerative (SAR) dose protocol (Murray and Wintle 2000, 2003) applied in this study.

step	SAR protocol
1	Dose
2	Preheat (220 °C; 10s)
3	Blue OSL (125 °C; 40s)
4	Test dose (17Gy)
5	Cutheat (180 °C)
6	Blue OSL (125 °C; 40s)
7	Blue OSL (280 °C; 40s)

Table 2. The specific radionuclide activities as well as the cosmic dose rates used for annual dose determination. It is assumed secular equilibrium between U and Ra. Specific activities were measured using high-resolution gamma spectrometry.

Sample code	Specific activities (Bq/kg)			Cosmic dose rate
	K-40	Th-232	Ra-226	
ZMN 55A	370±12	38±2	42±3	0.212±0.032
ZMN 65A	324±10	38±3	37±1	0.206±0.031
ZMN 75A	301±10	34±3	36±1	0.201±0.030
ZMN 85A	374±14	36±3	35±2	0.197±0.030
ZMN 95A	369±11	31±3	27±2	0.193±0.029

Table 3. Summary of the SAR-OSL ages. The age uncertainties were determined following **Aitken and Aldred (1972)**. The uncertainties associated with the luminescence and dosimetry data are random; the uncertainties mentioned on the optical ages are the overall uncertainties. The ages were calculated considering $15\pm 4\%$ water content.

Sample code	Depth (cm)	Equivalent dose (Gy)	Total dose rate (Gy/ka)	Age (ka)
ZMN 55A	55	14±2	2.6±0.06	5.4±0.7
ZMN 65A	65	16±2	2.3±0.04	6.8±0.9
ZMN 75A	75	21±2	2.2±0.06	9.3±1.2
ZMN 85A	85	20±3	2.4±0.07	8.4±1.4
ZMN 95A	95	16±2	2.2±0.06	7.4±1.0

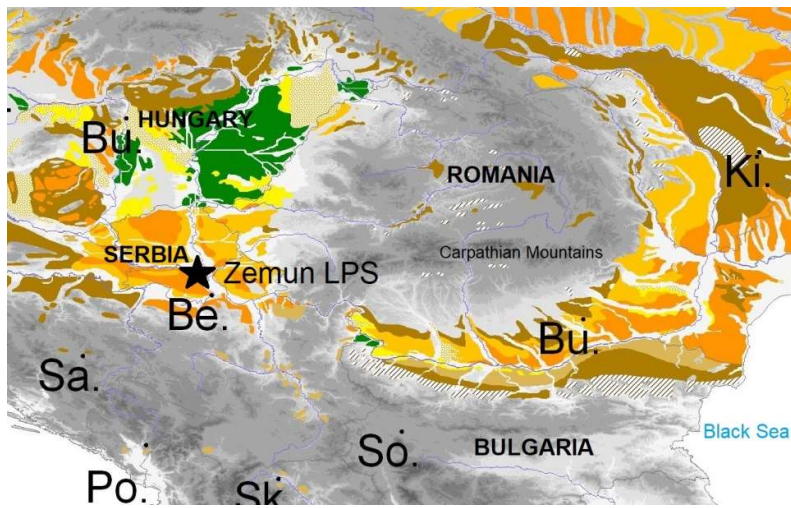


Fig. 1. The loess-paleosol sequence investigated in this study is represented by a star symbol and is integrated in the map of loess distribution after **Haase et al. (2007)**.

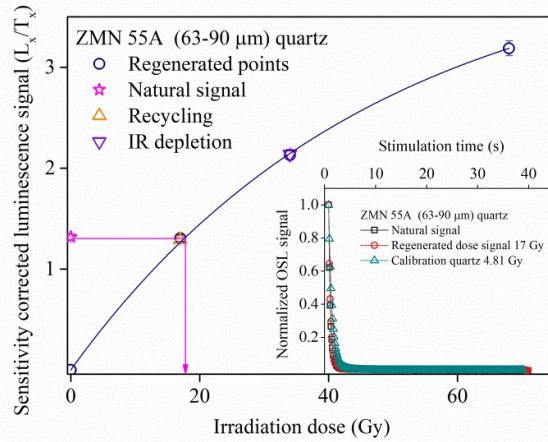


Fig. 2. Representative sensitivity-corrected dose response curve constructed for sample ZMN 55A using one aliquot of coarse quartz. The sensitivity corrected natural signal (star symbol) is interpolated on the dose response curve. IR depletion point is presented as an inverse triangle while Recycling point is depicted by an up triangle. The inset shows the pattern of a typical quartz decay curve which is compared with the decay of a regenerative dose as well as with the OSL decay of calibration quartz.

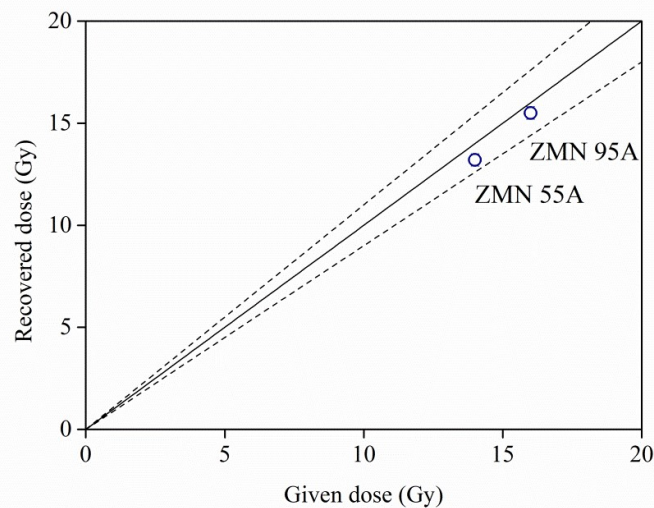


Fig. 3. Dose recovery test results for 63-90 μm quartz using SAR protocol. The given irradiation doses were chosen to be similar with the equivalent dose for each sample. The solid line indicates the ideal 1:1 dose recovery ratio while dashed lines indicate a 10% variation from unity.

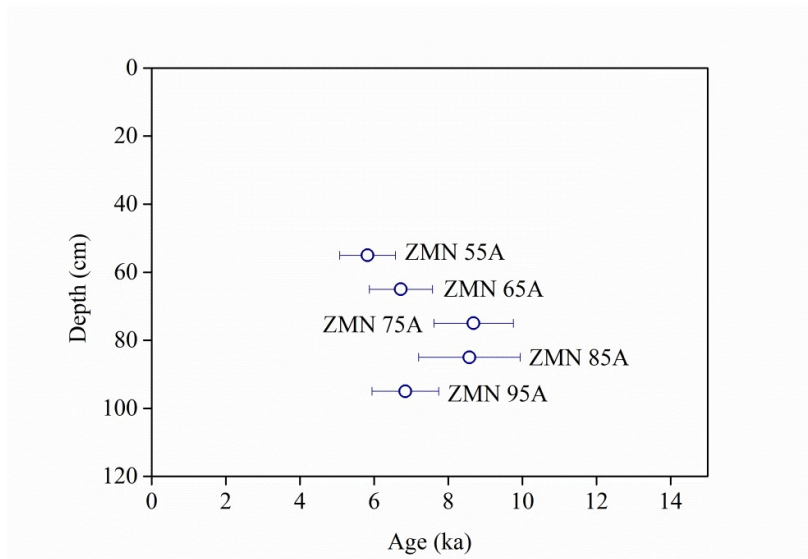


Fig. 4. Luminescence ages obtained on coarse quartz extracted from Zemun samples plotted as function of depth.